BIOMOLECULES & THERAPEUTICS

Original Article
Biomol Ther 32(3), 309-318 (2024)

Quinic Acid Alleviates Behavior Impairment by Reducing Neuroinflammation and MAPK Activation in LPS-Treated Mice

Yongun Park[1], Yunn Me Me Paing[1], Namki Cho[2], Changyoun Kim[3], Jiho Yoo[1], Ji Woong Choi[4] and Sung Hoon Lee[1,*]

[1]*College of Pharmacy, Chung-Ang University, Seoul 06974,*
[2]*Research Institute of Pharmaceutical Sciences, College of Pharmacy, Chonnam National University, Gwangju 61186, Republic of Korea*
[3]*Molecular Neuropathology Section, Laboratory of Neurogenetics, National Institute on Aging, National Institutes of Health, Bethesda, MD 20892, USA*
[4]*College of Pharmacy and Gachon Institute of Pharmaceutical Sciences, Gachon University, Incheon 21936, Republic of Korea*

Abstract

Compared to other organs, the brain has limited antioxidant defenses. In particular, the hippocampus is the central region for learning and memory and is highly susceptible to oxidative stress. Glial cells are the most abundant cells in the brain, and sustained glial cell activation is critical to the neuroinflammation that aggravates neuropathology and neurotoxicity. Therefore, regulating glial cell activation is a promising neurotherapeutic treatment. Quinic acid (QA) and its derivatives possess anti-oxidant and anti-inflammatory properties. Although previous studies have evidenced QA's benefit on the brain, *in vivo* and *in vitro* analyses of its anti-oxidant and anti-inflammatory properties in glial cells have yet to be established. This study investigated QA's rescue effect in lipopolysaccharide (LPS)-induced behavior impairment. Orally administering QA restored social impairment and LPS-induced spatial and fear memory. In addition, QA inhibited proinflammatory mediator, oxidative stress marker, and mitogen-activated protein kinase (MAPK) activation in the LPS-injected hippocampus. QA inhibited nitrite release and extracellular signal-regulated kinase (ERK) phosphorylation in LPS-stimulated astrocytes. Collectively, QA restored impaired neuroinflammation-induced behavior by regulating proinflammatory mediator and ERK activation in astrocytes, demonstrating its potential as a therapeutic agent for neuroinflammation-induced brain disease treatments.

Key Words: Quinic acid, Cognition, Social behavior, Neuroinflammation, Astrocytes, Extracellular signal-regulated kinase

INTRODUCTION

Neuroinflammation and oxidative stress initiate or encourage the neuropathology of neurodegenerative diseases. Glial cells are crucial for neuroinflammation in the brain as they release several proinflammatory mediators and reactive oxygen species (ROS) that aggravate neurotoxicity (Reynolds *et al*., 2007). Sustained glial cell activation induces excessive and chronic neuroinflammation, exacerbating neuropathology progression and development. Thus, reactive glial cell regulation is vital for inhibiting neuroinflammation-induced initiation or neurotoxicity propagation. Several agents have been fashioned to inhibit or regulate inflammation and oxidative damage in the brain. In particular, ethnopharmacological medicines with anti-inflammatory properties have garnered attention for their efficacy and safety (Jantan *et al*., 2015).

Given that herbal medicines can safely and efficiently regulate many inflammatory pathway factors (Koeberle and Werz, 2014), numerous natural plant products have been considered for inflammatory or neurodegenerative disease treatments (Bajda *et al*., 2011). For example, the neuroprotective effects and underlying mechanisms of quinic acid (QA) have been elucidated in previous *in vitro* studies. QA protects against glutamate-induced neurotoxicity by reducing oxidative stress (Rebai *et al*., 2017) and Aβ-induced neuronal cell death through inflammatory response suppression (Lee *et al*., 2018). QA derivatives also repress ROS production by inhibiting monoamine oxidase activity in neurons and astrocytes

Open Access **https://doi.org/10.4062/biomolther.2023.184**

Received Oct 25, 2023 **Revised** Dec 12, 2023 **Accepted** Dec 27, 2023
Published Online Apr 9, 2024

***Corresponding Author**
E-mail: sunghoonlee@cau.ac.kr
Tel: +82-2-820-5675, Fax: +82-2-815-0054

(Lim *et al*., 2020).

Furthermore, *in vivo* analyses highlighted the protective role of QA in the brain disease animal model. Although blood-brain barrier penetration through natural products is limited, previous behavioral results indicate that QA may penetrate the blood-brain barrier for neuroprotection. For instance, oral QA administration reduced aluminum chloride-induced memory deficit (Liu *et al*., 2020) and ameliorated memory impairment in Alzheimer's disease animal models (Kwon *et al*., 2016). In addition, dietary QA derivatives reduce stress hormone-induced depressive behavior (Lim *et al*., 2020). Gallic acid was also detected in brain tissues after repeated oral exposure (Ferruzzi *et al*., 2009), and protocatechuic acid was localized in brain micro-dialysates post-peripheral exposure (Zhang *et al*., 2011).

Although the beneficial role of QA in the brain has been previously reported, an *in vivo* analysis of QA's anti-inflammatory properties in glial cells has yet to be established. Our previous study concluded that neuroinflammation induced cognition and social behavior impairments (Kim *et al*., 2022). Therefore, this study investigates the protective effect of QA against neuroinflammation-induced behavioral impairment by suppressing glial cell activation. We discovered that oral QA administration protects against neuroinflammation-induced behavioral impairment, evidencing that QA is a bioactive molecule in the brain.

MATERIALS AND METHODS

Materials

Antibodies and reagents were obtained from the manufacturers as follows: Thermo Fisher Scientific, MA, USA—LPS serotype 055:B5, 4-Hydroxynonenal (4-HNE), diamidino-2-phenylindole (DAPI), DMEM F12, penicillin-streptomycin, trypsin-EDTA, opti-MEM™, and Lipofectamine LTX Reagent with PLUS™ Reagent; Merck, CA, USA—QA; BD Biosciences, NJ, USA—inducible nitric oxide synthase (iNOS) and p65; Santa Cruz Biotechnology, CA, USA—cyclooxygenase-2 (COX-2), β-actin, IκBα, and Histone H3; Cell Signaling Technology, MA, USA—p-extracellular signal-regulated kinase (ERK), ERK, p-JNK, c-Jun N-terminal kinase (JNK), p-p38, and p38; Abcam, Cambridge, UK—glial fibrillary acidic protein (GFAP), Alexa Fluor 488®-, and Alexa Fluor 594®-conjugated secondary antibodies; and Young In Frontier, Seoul, Korea—fetal bovine serum (FBS).

Animal care and drug treatment

Male C57BL/6 mice (25 g) were purchased from Nara-Biotec (Seoul, Korea). All animal experiments adhered to the laboratory animal care principles and were approved by the Institutional Animal Care and Use Committee of Chung-Ang University (protocol number: 2020-00049). Mice were kept in a 12-h light/dark cycle environment at 22 ± 3°C with ad libitum access to food and water.

Mice were randomly divided into vehicle (Veh, n=6), LPS (n=6), and LPS+QA groups (n=6 for QA 10 mg/kg and n=6 for QA 50 mg/kg). LPS and QA were dissolved in Dulbecco's phosphate-buffered saline (DPBS) and ethanol. The Veh group was orally treated with ethanol and injected with the same volume of DPBS as the QA; the QA group was orally administered 10 and 50 mg/kg QA for five consecutive days. The QA dosage was determined by previous studies (Kwon *et al*., 2016; Lim *et al*., 2020). The LPS injection was administered as reported previously but slightly modified (Kim *et al*., 2022). Mice were anesthetized with an isoflurane–O2 (2:1.4) mixture and placed on a stereotaxic frame. LPS was infused intracerebroventricularly (i.c.v.; 30 μg in 3 μL) into the lateral ventricle (−0.38 mm anteroposterior, −1.0 mm mediolateral, and −2.4 mm dorsoventral) using a Hamilton microsyringe (Hamilton company, NV, USA) with a 26-gauge needle for a 1-2 min diffusion period before needle withdrawal.

Y-maze test

The spontaneous alternation behavioral test in the Y-maze was performed as detailed in our previous study. The maze comprised three white acrylic arms (40×14×4 cm, length×height×width) at the bottom and 10 cm high wide at the top. Mice were placed at one arm's end and freely explored the maze during a 10-min session. Mice movements were recorded, and alternation was analyzed with EthoVision software (Noldus, Wageningen, The Netherlands). 'Arm entry' was determined when all four paws were successfully placed within one arm, and 'alternation' was defined as successive entry into the three arms on overlapping triplet sets. The alternation percentage was calculated using the following equation:

$$\text{Alternation (\%)} = \left(\frac{\text{Actual Alternation}}{\text{Total Arm Entries-2}} \right) \times 100$$

'Direct revisits' was defined as the number of consecutive visits in a single arm. 'Traveled distance' and the 'number of entries' were automatically analyzed through EthoVision software. All mazes were cleaned with 70% ethanol and dried before and after each trial.

Barnes maze test

The Barnes maze test was performed on a white circular platform (70 cm in diameter) with 15 holes (5 cm in diameter) equally spaced around the perimeter. The platform was elevated 80 cm above the floor, and spatial cues were marked on the room's walls. The mouse was initially positioned at the maze's center and trained to enter the black escape box (9×9×20 cm, length×height×width) beneath the holes, ending the trial. The maze was rotated daily, though spatial location cues remained consistent. Mice were trained to find the holes during the training session, and four consecutive acquisition trials were recorded using computerized tracking software (EthoVision XT, Noldus) with at least 30 min for rest.

Radial-arm maze test

Spatial working memory tasks were evaluated through radial-arm maze tests. The radial maze was constructed from transparent plastic elevated 80 cm above the floor. The octagonal central platform (21 cm) was surrounded by a wall (7 cm), and each arm (25 cm) radiated from the platform. The maze was placed in a room with several extra-maze cues. The mouse was deprived of food by maintaining 80-90% of body weight during the pre-training, training, and trial sessions. During pre-training, the mouse was placed on the central platform to explore the maze freely and find the scattered food pellets for 15 min. In the training session, four arms were baited with food pellets, and the mouse was encouraged to find the four food pellets at each arm's end; training finished when the

mouse consumed the food pellets. For the acquisition trial, the mouse was placed on the central platform and allowed to consume the four food pellets. Trials were performed once daily, the video camera was fixed above the maze, and the total error ratio for each trial was calculated (EthoVision XT, Noldus).

Passive avoidance tests

Passive avoidance tests were performed as previously described (Pittenger *et al*., 2006). Light–dark passive avoidance tests were conducted in a passive-avoidance box with two compartments, one dark and one bright chamber (white and illuminated by an 8 W bulb) connected by a door. During training sessions, the mouse was initially placed in the bright chamber. The door automatically closed once the mouse crossed into the dark chamber, and the mouse subsequently received an electrical foot shock (3 s at 0.3 mA). The time spent in the light chamber was measured. One day after the training session, the mouse was tested in the passive avoidance box under the same conditions, excluding the electrical foot shock.

Step-through passive avoidance tests were performed in a box (21×20×20 cm, length×height×width) with an elevated round platform (7 cm diameter) in the center of an electrical grid floor. The mouse was first placed on the platform during training. When the mouse stepped down and put all paws onto the grid, a 0.4 mA electrical shock was applied for 9 s. At 24, 48, and 72 h after training, the mouse was again placed on the platform, and the time spent on the platform was measured. A retention time of more than 300 s was cut off.

Three-chamber test

Social behavior, sociability, and social novelty were quantified through a three-chamber test. The three-chamber apparatus was made of white acrylic (63×23×42 cm, length×height×width) and three different chambers with small, round open doors for free access to other chambers. The social behavior procedure entailed habituation, sociability, and social novelty. During habituation, the mouse was placed in the middle chamber for 10 min and allowed free access to other chambers, each containing an empty wire cup. During the sociability phase, a stranger mouse (8 weeks old, same-sex, Stranger 1) was placed in one side chamber, and an empty wire cup (Object) was placed on the opposite side. The subject mouse was allowed to explore the chamber, and movement was tracked for 10 min. The social novelty phase followed the sociability test; a new stranger mouse (Stranger 2) replaced the empty wire cup, and the subject mouse was allowed to explore the chambers for 10 min. The time spent in each compartment was automatically tracked by a camera and analyzed using Ethovision software. Sociability and social novelty scores were calculated as follows:

$$\text{Sociability score (\%)} = \left(\frac{(\text{Time}_{\text{stranger}} - \text{Time}_{\text{object}})}{(\text{Time}_{\text{stranger}} + \text{Time}_{\text{object}})} \right) \times 100$$

$$\text{Social novelty score (\%)} = \left(\frac{(\text{Time}_{\text{stranger 2}} - \text{Time}_{\text{stranger 1}})}{(\text{Time}_{\text{stranger 1}} + \text{Time}_{\text{stranger 2}})} \right) \times 100$$

Open-field test

The open-field test assessed anxiety and locomotor behavior using a white acrylic box (40×40×40 cm, length×height×width) subdivided into center and outer zones through automatic tracking software. Each mouse was allowed to explore the area freely for 5 min. The total distance traveled and time spent (%) in the center were monitored.

Western blot

Total protein lysates from the hippocampus (n=4 in each group) or cells (n=3 independent cultures) were extracted with a radioimmunoprecipitation assay (RIPA) buffer (Biosesang, Inc., Yongin, Korea) containing a protease and phosphatase inhibitor cocktail (Roche, Basel, Switzerland); the concentration was measured using bovine serum albumin (BSA). Proteins were denatured after boiling at 95°C for 15 min, and 20-30 μg of protein was separated through electrophoresis. Proteins were transferred onto a nitrocellulose membrane (Whatman, NJ, USA) and incubated overnight with primary antibodies at 4°C. Then, membranes were incubated with secondary antibodies conjugated to horseradish peroxidase for 1 h at 15-25°C. Protein bands were detected using an enhanced chemiluminescence (iNtRON Biotechnology, Seongnam, Korea) reagent and visualized with a chemiluminescence system (Vilber, Collégien, France).

Cell culture and treatment

Primary astrocytes were cultured following a previously described method (Kim *et al*., 2022). Sprague Dawley (SD) rats were purchased from Young Bio (Seongnam, Korea), and cerebral hippocampi from postnatal 1-day-old pups were collected for mechanical dissociation. Cultures were plated in a T75 flask in DMEM F12 with 10% FBS, 100 μg/mL streptomycin, and 100 U/mL penicillin. Fresh medium was replaced every two to three days, and the cells were grown over seven. Cells were subcultured with 0.25% trypsin-EDTA and seeded onto poly-D-lysine (PDL)-coated plates for further experimentation. Cells were pretreated with vehicle (Veh) or DMSO 1 h before LPS (10 ng/mL), and the Veh group was treated with 0.1% DMSO.

Nitrite assay

Nitrite release was assessed with the Griess reagent (0.1% naphthyl ethylenediamine and 1% sulfanilamide in 5% H_3PO_4). Cells were left untreated or treated with LPS for 24 h, and the supernatant was collected and incubated with the same Griess reagent volume for 5 min at 15-20°C. Absorbance was measured using a microplate reader (BioTek Instruments, VT, USA) at 540 nm, and the nitrite concentration was determined through a standard NaNO2 curve.

Cell viability

Cellular toxicity was measured with a tetrazolium salt 3-(4, 5-dimethylthiazol-2-yl)-2, 5-diphenyltetrazolium bromide (MTT, Sigma, MO, USA). Cells were incubated with 100 μg/mL MTT reagent for 1 h at 37°C, and formazan crystals were dissolved in DMSO. Absorbance was measured at 540 nm using a microplate reader (BioTek Instruments).

Reverse transcription-polymerase reaction (RT-PCR)

iNOS and GAPDH mRNA were extracted with a Trizol Reagent (Thermo Fisher Scientific), and cDNA was synthesized using the GoScript™ Reverse Transcriptase (Promega, WI, USA). PCR amplification followed the standard polymerase protocol (Promega). The PCR primer sequences were as follows: iNOS forward (5-GAG GTA CTC AGC GTG CTC CA-

Table 1. Results of statistical analysis

		ANOVA			
	Figs	Interaction	Main effect	*F* (DFn, DFd)	*p*-value
Fig. 1B	% of alternation		Treatment	$F_{(3, 20)}$=26.160	<0.001
	Number of direct revisits		Treatment	$F_{(3, 20)}$=13.930	<0.001
	Total distance		Treatment	$F_{(3, 20)}$=0.365	0.780
	Number of entries		Treatment	$F_{(3, 20)}$=1.434	0.260
Fig. 1C		Treatment×Number of trial		$F_{(9, 72)}$=0.748	0.660
			Treatment	$F_{(3, 72)}$=19.130	<0.001
			Number of trial	$F_{(3, 72)}$=88.910	<0.001
Fig. 1D		Treatment×Number of trial		$F_{(12, 100)}$=1.837	0.050
			Treatment	$F_{(3, 100)}$=20.530	<0.001
			Number of trial	$F_{(4, 100)}$=58.440	<0.001
Fig. 2A		Treatment×Day		$F_{(3, 40)}$=13.420	<0.001
			Treatment	$F_{(3, 40)}$=13.520	<0.001
			Day	$F_{(1, 40)}$=187.100	<0.001
Fig. 2B		Treatment×Day		$F_{(9, 80)}$=5.044	<0.001
			Treatment	$F_{(3, 80)}$=18.720	<0.001
			Day	$F_{(3, 80)}$=111.600	<0.001
Fig. 3A	Sociability	Treatment×Chamber		$F_{(3, 40)}$=9.062	0.001
			Treatment	$F_{(3, 40)}$=1.907	0.144
			Chamber	$F_{(1, 40)}$=81.530	<0.001
	Sociability score		Treatment	$F_{(3, 20)}$=19.790	<0.001
Fig. 3B	Social novelty	Treatment×Chamber		$F_{(3, 40)}$=6.760	<0.001
			Treatment	$F_{(3, 40)}$=0.740	0.534
			Chamber	$F_{(1, 40)}$=73.320	<0.001
	Social novelty score		Treatment	$F_{(3, 20)}$=11.760	<0.001
Fig. 4A			Treatment	$F_{(3, 20)}$=16.290	<0.001
Fig. 4B			Treatment	$F_{(3, 20)}$=0.6476	0.593
Fig. 5		Treatment×Protein		$F_{(15, 72)}$=5.487	<0.001
			Treatment	$F_{(3, 72)}$=116.700	<0.001
			Protein	$F_{(5, 72)}$=13.720	<0.001
Fig. 6A			Treatment	$F_{(4, 35)}$=12.220	<0.001
Fig. 6B			Treatment	$F_{(4, 38)}$=3.763	0.011
Fig. 7	p-ERK		Treatment	$F_{(4, 10)}$=13.330	<0.001
	p-JNK		Treatment	$F_{(4, 19)}$=3.321	0.031
	p-p38		Treatment	$F_{(4, 19)}$=25.540	<0.001

3) and reverse (5-AGG GAG GAA AGG GAG AGA GG-3); GAPDH forward (5-CCA GTA GAC TCC ACT CAC G-3) and reverse (5-CCT TCC ACA ATG CCA AAG TT-3).

Immunocytochemistry

Cells were plated on PDL-coated coverslips, fixed with 4% paraformaldehyde for 15 min, and treated with 0.1% Triton for 10 min at 15-25°C for immunochemistry. The coverslips were incubated at 4°C overnight with a blocking solution containing primary antibodies. Then, coverslips were incubated with Alexa Fluor 488®- and Alexa Fluor 594®-conjugated secondary antibodies. Nuclei were stained with DAPI, and coverslips were mounted with gel mount solution (Biomeda, CA, USA). Cells were visualized with a confocal microscope (LSM 800, Zeiss, Oberkochen, Germany).

Statistical analyses

Data are expressed as the mean ± standard error of the mean (SEM) for at least three independent experiments. Statistical significance was determined through the Mann-Whitney test for nonparametric tests, one-way analysis of variance (ANOVA) followed by post-hoc Tukey's test, or two-way ANOVA followed by post-hoc Bonferroni's test for intergroup comparisons using GraphPad Prism 5 (GraphPad Software, Inc., CA, USA). Table 1 details the statistical analysis results, including *F*-value, degree of freedom, and *p*-value. *p*-values less than 0.05 were considered statistically significant.

RESULTS

QA attenuates LPS-induced spatial memory impairment in mice

In our previous study, neuroinflammation induced through LPS administration reduced learning, memory, and social interactions (Kim *et al*., 2022). Therefore, QA was orally administered in mice once daily for five consecutive days to investigate the protective effect of QA against neuroinflammation. Since LPS cannot penetrate the blood-brain barrier, LPS was injected into the hippocampus (i.c.v., 30 μg/mouse).

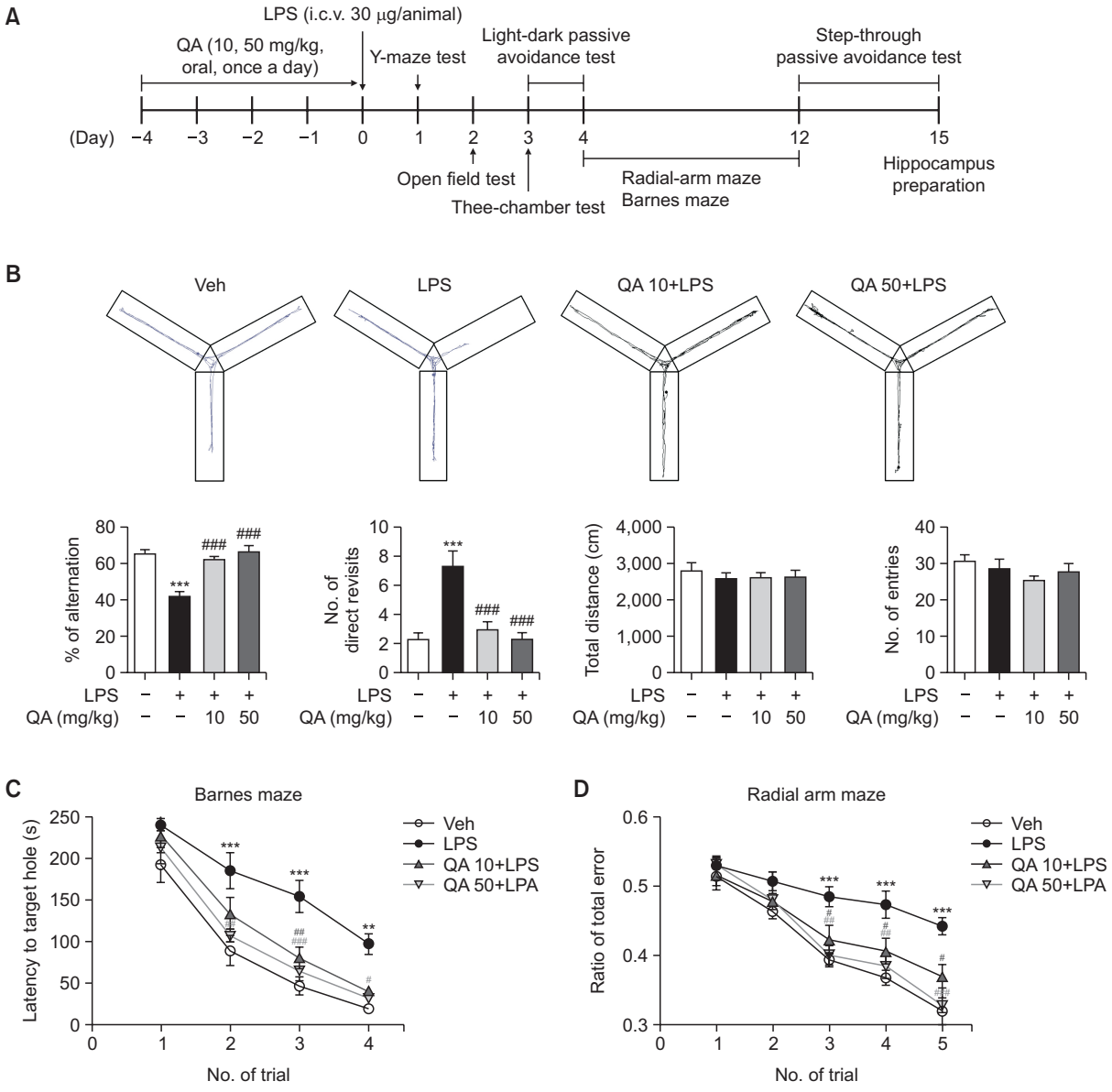

Fig. 1. QA administration alleviated LPS-induced spatial memory impairment. (A) Experimental scheme schedule. Daily oral QA administration (10 and 50 mg/kg) over five days, and i.c.v LPS injection into the mouse hippocampus. Spatial memory evaluation through Y-maze, Barnes maze, and radial maze tests; fear memory with light-dark and step-down avoidance tests. Social behavior assessment through the three-chamber tests. (B) Y-maze results. Representative traces of mouse tracking in each group (upper) and summary bar graphs of alternation rate, direct revisits, total movement, and entries (lower). ***p<0.001 compared to Veh; $^{###}p$<0.001 compared to Veh+LPS. (C) Barnes maze test; latency to find the target hole in each group during repeat testing. (D) Radial arm maze test; error ratio to find all the food in each group. **p<0.01 and ***p<0.001 compared to each day of Veh; $^{#}p$<0.05, $^{##}p$<0.01, and $^{###}p$<0.001 compared to each day of Veh+LPS.

Mice were euthanized after the behavioral analyses, and hippocampal tissues were dissected for further study (Fig. 1A). Spatial memory was assessed through the Y-maze, Barnes maze, and radial arm maze tests. The Y-maze test results revealed that LPS injection decreased alternation (%) and direct revisits, indicating that neuroinflammation diminished cognitive behavior. In addition, Y-maze results attested that QA treatment restored LPS-induced spatial memory impairment but did not affect total distance or entries (Fig. 1B). The total distance and entries were similar in all groups. In the Barnes maze test, Veh and LPS groups displayed a gradual latency decrease to the target hole. However, LPS-injection elevated latency to the target hole more than Veh in each trial (Fig. 1C). QA treatment reduced latency in LPS-injected mice. Similarly, QA significantly attenuated the LPS-induced higher error ratio in the radial-arm test (Fig. 1D).

QA alleviates LPS-induced fear memory impairment in mice

Next, passive avoidance tests were conducted to evaluate fear learning and memory in mice (Kameyama *et al*., 1986). Light-dark passive avoidance tests showed that the entry la-

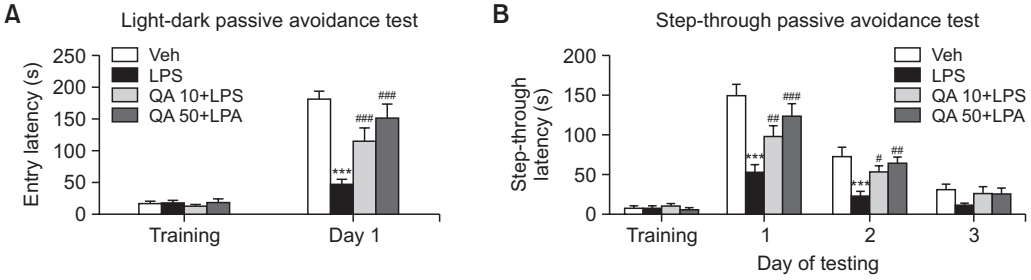

Fig. 2. QA attenuated LPS-induced fear memory impairment. (A) Light-dark avoidance test; entry latency to the light chamber during training and trial sessions. (B) Step-through down avoidance test; latency in each group from Day 1 to 3 of the trial sessions. ***p<0.001 compared to each day of Veh; $^{\#}p$<0.05, $^{\#\#}p$<0.01, and $^{\#\#\#}p$<0.001 compared to each day of Veh+LPS.

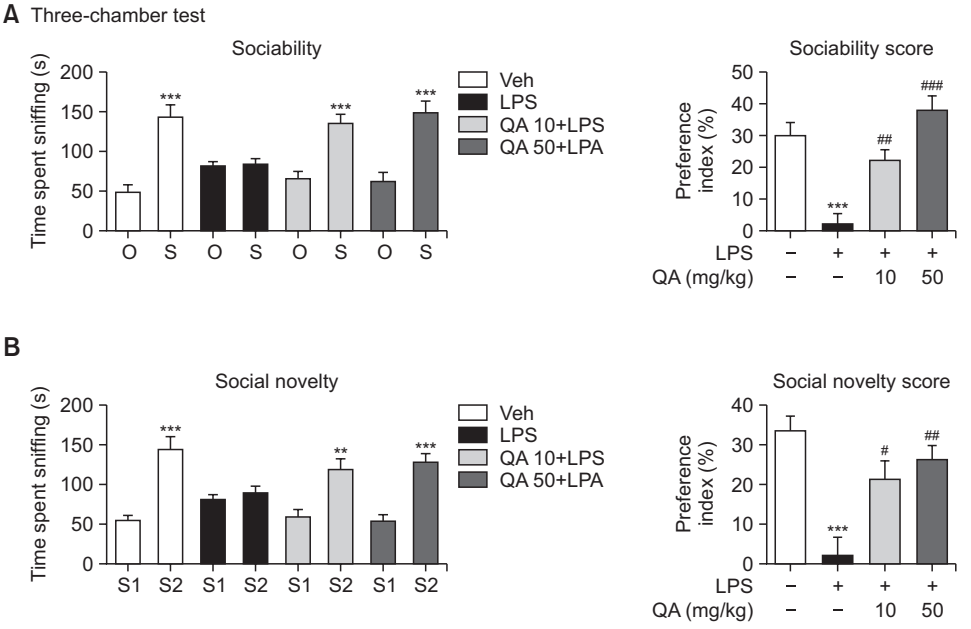

Fig. 3. QA ameliorated LPS-induced social deficit. (A, B) Sociability and social novelty tests using the three-chamber test. Sociability and social novelty score calculations based on the duration time in each chamber: n=5 (Veh), 6 (Veh+LPS), 6 (QA 10+LPS), and (QA 50+LPS) mice. ***p<0.001 compared to Veh, and $^{\#}p$<0.05, $^{\#\#}p$<0.01, and $^{\#\#\#}p$<0.001 compared to Veh+LPS in score.

tency into the dark room was lower in LPS-injected mice than in Veh. However, this latency time was restored by QA administration (Fig. 2A). In addition, latency was gradually reduced in repeat trials of the step-through passive avoidance test (Fig. 2B). QA administration attenuated the latency reduction from LPS (Fig. 2B).

QA rescues LPS-induced social deficit in mice

Next, sociability and social novelty were measured through the three-chamber test to explore QA's effect on social interaction. During the sociability test, Veh mice spent significantly more time in the Stranger 1 chamber than with the Object, whereas LPS-injected mice spent a similar time in both (Fig. 3A). QA-exposed mice spent significantly more time with Stranger 1 than the Object, indicating that QA treatment restored sociability. For the social novelty test, Veh mice spent more time in the Stranger 2 chamber than Stranger 1, whereas LPS-injected mice spent a comparable time in both (Fig. 3B). Lastly, QA-treated mice spent significantly more time with Stranger 2 than Stranger 1, suggesting that QA can restore neuroinflammation-induced social novelty deficit. These results substantiate that QA protects against LPS-induced social impairment in mice.

Effects of QA on LPS-induced anxiety and locomotor in mice

Time spent in the center zone was measured during the open field test to investigate the effect of QA on anxiety. LPS-injected mice spent less time in the center zone than in Veh, and QA did not induce any significant change compared to LPS-injected mice (Fig. 4A). These results indicated that QA marginally affects LPS-induced anxiety behavior. Additionally, the total traveled distance was similar across all groups (Fig. 4B), suggesting LPS did not induce locomotor deficit.

Effects of QA on LPS-induced proinflammatory mediator expressions and MAPK activation in the LPS-injected hippocampus

The behavioral impairment induced by proinflammatory cytokines during neuroinflammation can be alleviated by inhibiting their expression (Zhao *et al*., 2019). iNOS produces extensive amounts of nitrite in response to an inflammatory stimulus, and COX-2 production mediates the neurotoxic effect in neuroinflammation. Therefore, we measured iNOS and COX-2 expressions in an LPS-injected hippocampus treated with or without QA. In addition, MAPK activation is associated with the LPS upregulation of proinflammatory mediator expressions in stimulated astrocytes. Thus, MAPK activation was investigated in the LPS-injected hippocampus since MAPK pathways influence iNOS and COX-2 expressions (Lu *et al*., 2010). Low QA doses (10 mg/kg) reduced iNOS expression and ERK phosphorylation without affecting COX-2 expression or JNK and p38 phosphorylation (Fig. 5). However, high QA doses (50 mg/kg) significantly repressed iNOS and COX-2 expressions and MAPK phosphorylation in the LPS-injected hippocampus. In addition, both low and high QA doses repressed 4-HNE expression, a lipid peroxidation product. These results suggest that QA restored the increased proinflammatory mediators, oxidative stress, and MAPK activation in the LPS-injected hippocampus.

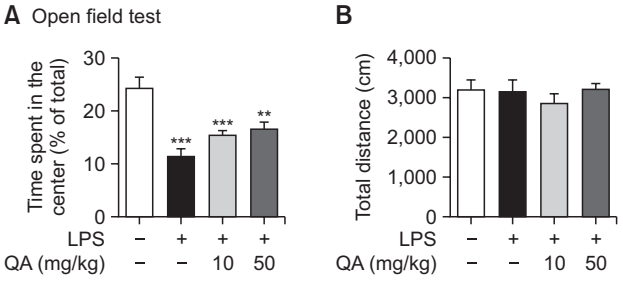

Fig. 4. Effects of QA on anxiety and locomotor behavior in mice. Open field test results. (A) Anxiety behavior from LPS injection was measured by the time ratio spent in the center area. QA did not affect LPS-induced anxiety behavior. (B) Traveled distance results. All groups exhibited similar locomotor behavior. ***p*<0.01 and ****p*<0.001 compared to Veh.

Effects of QA on nitrite release and nuclear p65 translocation in LPS-stimulated astrocytes

Astrocytes are predominant glial cells crucial to brain inflammation as they release proinflammatory cytokines. Therefore, LPS-stimulated primary astrocytes were exposed to QA to identify the cells contributing to its anti-inflammatory effect on the LPS-injected brain. We investigated the effect of QA on nitrite release, a representative proinflammatory mediator in LPS-stimulated astrocytes. QA repressed the nitrite release at the indicated concentrations in LPS-stimulated astrocytes without cytotoxicity (Fig. 6A, 6B). Next, the effect of QA on iNOS protein expression was examined in LPS-stimulated astrocytes. Consistent with the LPS-injected hippocampus results, QA significantly inhibited LPS-induced iNOS expression (Fig. 6C). Furthermore, QA significantly reduced the LPS-induced upregulation of iNOS mRNA expression (Fig. 6D).

Nuclear p65 translocation promotes proinflammatory mediator transcription and is regulated by IκB during inflammation. Therefore, regulating the translocation of p65 into the nucleus mediates these anti-inflammatory effects (Kim and Shin, 2006). QA's regulatory effect on the nuclear translocation of p65 was examined using immunocytochemistry. QA treatment repressed LPS-induced translocation of p65 into the nucleus (Supplementary Fig. 1). These results indicated that QA has anti-inflammatory influence in the LPS-injected brain by controlling proinflammatory mediator expression and the nuclear translocation of p65 in astrocytes.

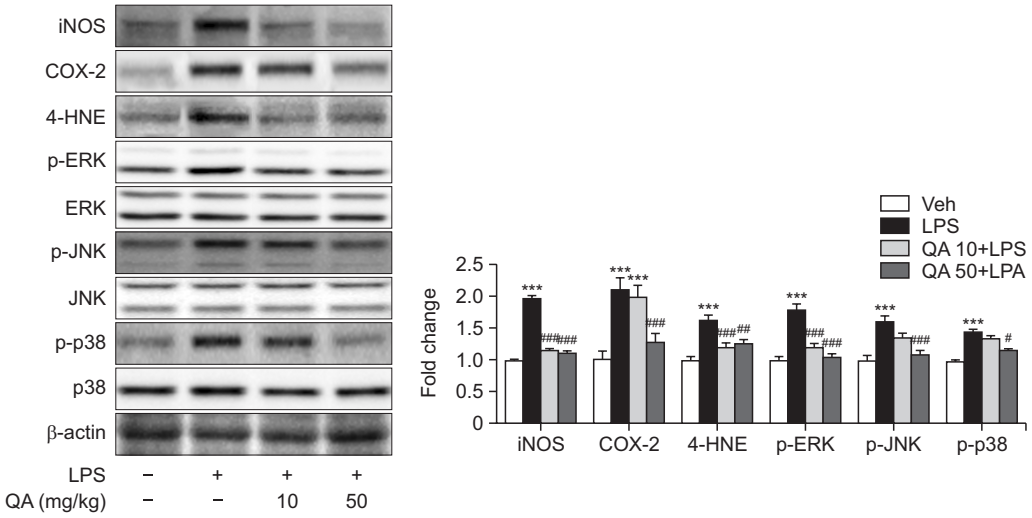

Fig. 5. QA inhibited LPS-induced proinflammatory mediator expression, oxidative stress marker elevation, and MAPK activation in the hippocampus. Protein expressions in the mouse hippocampus. QA alleviated iNOS, COX-2, and 4-HNE expressions and MAPK phosphorylation in the LPS-injected hippocampus. MAPK phosphorylation was normalized with total MAPK (n=5-7). ****p*<0.001 compared to Veh; #*p*<0.05, ##*p*<0.01, and ###*p*<0.001 compared to Veh+LPS.

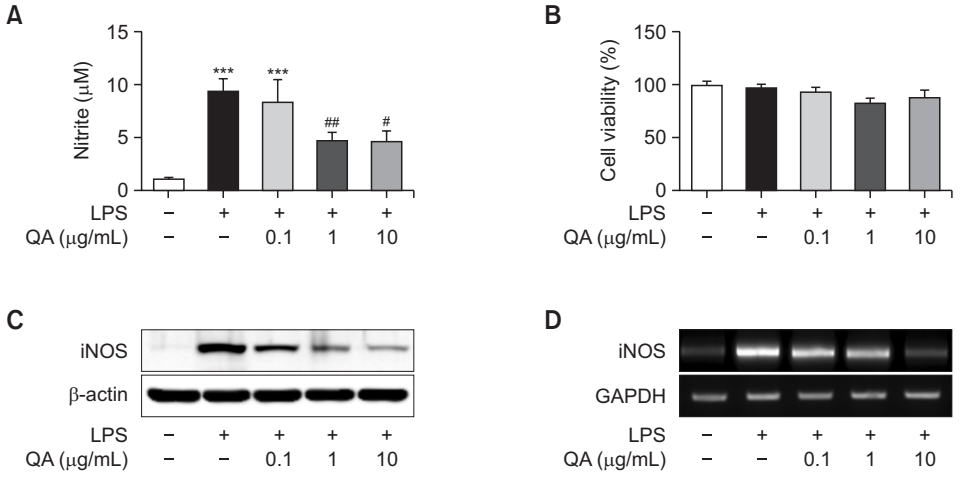

Fig. 6. QA effects on iNOS expression in LPS-stimulated primary astrocytes. Primary astrocytes were treated with or without QA at the indicated doses 2 h before LPS treatment (10 ng/mL). (A) Nitrite level incubation with LPS for 24 h. (B) Cell viability through MTT assay. (C) iNOS protein expressions in astrocytes incubated with LPS for 24 h. iNOS blots were normalized with those of β-actin. (D) iNOS mRNA expressions after 6 h of incubation with LPS. iNOS mRNA expressions were normalized with those of GAPDH. ***p<0.001 compared to Veh; $^{\#}p$<0.05 and $^{\#\#}p$<0.01 compared to Veh+LPS.

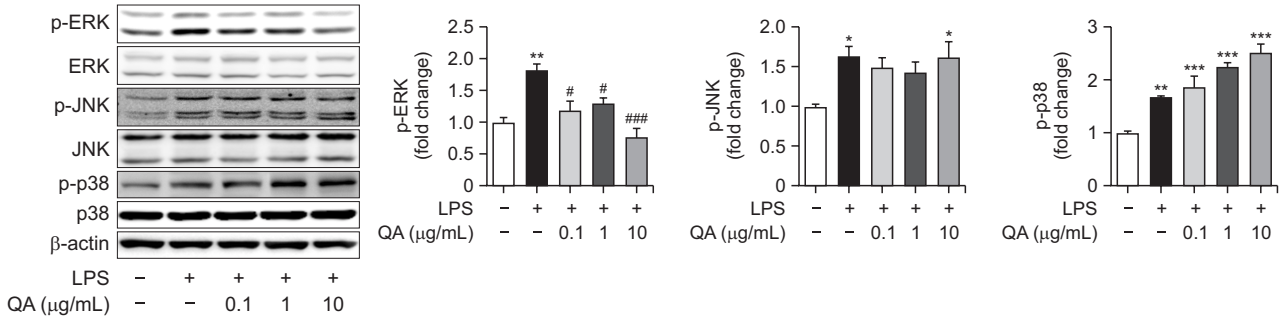

Fig. 7. QA effects on LPS-induced MAPK activation in astrocytes. QA application 2 h before LPS treatment. Total and phosphorylated MAPK protein expressions after 2 h of LPS incubation. LPS elevated MAPK phosphorylation, and QA reduced p-ERK. Phosphorylated MAPK was normalized with total MAPK. *p<0.05, **p<0.01, and ***p<0.001 compared to Veh; $^{\#}p$<0.05 and $^{\#\#\#}p$<0.001 compared to Veh+LPS.

Effects of QA on MAPK activation in LPS-stimulated primary astrocytes

To further investigate the effect of QA on MAPK activation, astrocytes were pretreated with various QA concentrations for 2 h and LPS for 24 h. As such, LPS enhanced MAPK activation, and QA attenuated ERK phosphorylation (Fig. 7). However, QA induced marginal changes in JNK and p38 phosphorylation.

DISCUSSION

Compared to other tissues, the brain has a low endogenous antioxidant defense (Halliwell, 2006); the hippocampus, the central learning and memory region, is particularly susceptible to oxidative stress (Huang *et al*., 2015). Elevated neuroinflammation and oxidative stress from LPS injection may preferentially repress the hippocampal neuronal activity that impairs learning and social behavior. In our current and previous studies, LPS administration reduced social behavior in mice alongside proinflammatory mediator upregulation in glial cells (Kim *et al*., 2022).

Astrocytes are abundant glial cells that mediate neuroinflammatory responses in the brain, and microglia release several of these inflammatory mediators (von Bartheld *et al*., 2016). Since this reaction is a self-amplifying inflammatory response to inflammatory cytokines and peroxidized lipids in glial cells (Glass *et al*., 2010), regulating glial cell activation is necessary to aggravate neuroinflammation-induced neuropathology. Notably, neurodegenerative diseases that induce cognitive impairment exhibit glial cell activation and proinflammatory cytokine overproduction (Kumar, 2018). In addition, a study using positron emission tomography revealed that glial cell activation may be associated with inflammation-induced social deficit (Sandiego *et al*., 2015). Therefore, regulating glial activation can alleviate neuroinflammation-induced behavioral impairment. Some plants and their bioactive compounds exhibit neuroprotective properties by regulating proinflammatory mediator expression in glial cells (Park *et al*., 2009).

The present study's behavioral analyses verified that oral

QA treatment ameliorated LPS-induced deficits in short- and long-term spatial memory, fear memory, and social behavior. QA dose-dependently suppressed proinflammatory mediator expression and the oxidative stress marker in LPS-injected hippocampus. In addition, QA restored the previously inhibited MAPK activation in the LPS-injected hippocampus. Although we could not quantify precise QA amounts in the hippocampal region, QA was proven to exert anti-inflammatory effects in the brain, alleviating behavior impairment.

In vitro analyses in the present study provided insights into the preventive effects of QA on iNOS expression and nuclear p65 translocation in astrocytes. iNOS is a calcium-independent NOS that produces excessive NO, which leads to neuronal damage and excitotoxicity from N-methyl-d-aspartate receptor activation (Calabrese *et al*., 2007). As NO stimulates the production of proinflammatory mediators that aggravate neuroinflammation, iNOS regulation in glial cells is essential for preventing inflammation-associated brain damage. Several studies have demonstrated that MAPK pathways regulate iNOS expression in glial cells in response to inflammatory stimuli (Saha and Pahan, 2006). In LPS-stimulated astrocytes, QA preferentially repressed ERK phosphorylation rather than JNK or p38 phosphorylation and nuclear translocation of p65.

The hippocampus comprises various cell types, such as astrocytes, microglia, neurons, and oligodendrocytes. Given cell-type specific MAPK activation in physiological and pathological conditions in mice brains (Bu *et al*., 2007; Bin Saifullah *et al*., 2018), the regulatory effect of QA on MAPK activation may differ in neural cells. Consistently, the regulatory effect's natural product on MAPK activation was different in the LPS-exposed hippocampus and astrocytes (Kim *et al*., 2022).

ERK hyperactivation has been linked to neurodegenerative diseases in the CNS, in which neuroinflammation is a hallmark of disease (Chitnis and Weiner, 2017). It has been shown that pharmacological ERK inhibition ameliorated inflammatory responses and neuronal apoptosis in mice brains (Wang *et al*., 2004; Liu *et al*., 2022). Thus, ERK has drawn attention as a potential therapeutic for neurodegenerative diseases by suppressing inflammatory responses (Lucas *et al*., 2022). In addition, ERK regulates iNOS expression and Nf-κB pathway activation (Chan and Riches, 2001; Zhang *et al*., 2012), which are critical in neuroinflammation and glial cell activation. In the present study, QA mediates the anti-inflammatory effect by regulating ERK phosphorylation, ameliorating the behavioral impairments in the LPS-exposed hippocampus.

CONFLICT OF INTEREST

The authors declare no conflicts of interest.

ACKNOWLEDGMENTS

This research was supported by the National Research Foundation of Korea (NRF) grant funded by the Korean Government (MSIT) (Grant No. 2020R1C1C1008852, 2021R1C1C1012076, 2021M3E5E3080529, and 2021R1A6A1A0304429).

AUTHOR CONTRIBUTIONS

Yongun Park: Methodology, Investigation. Yunn Me Me Paing: Methodology, Validation. Namki Cho: Conceptualization, Writing – review, editing. Changyoun Kim: Validation, Supervision. Jiho Yoo: Resources, Writing – review, editing. Ji Woong Choi: Data curation, Conceptualization. Sung Hoon Lee: Conceptualization, Writing.

REFERENCES

Bajda, M., Guzior, N., Ignasik, M. and Malawska, B. (2011) Multi-target-directed ligands in Alzheimer's disease treatment. *Curr. Med. Chem.* **18**, 4949-4975.

Bin Saifullah, M. A., Nagai, T., Kuroda, K., Wulaer, B., Nabeshima, T., Kaibuchi, K. and Yamada, K. (2018) Cell type-specific activation of mitogen-activated protein kinase in D1 receptor-expressing neurons of the nucleus accumbens potentiates stimulus-reward learning in mice. *Sci. Rep.* **8**, 14413.

Bu, X. N., Huang, P., Qi, Z. F., Zhang, N., Han, S., Fang, L. and Li, J. F. (2007) Cell type-specific activation of p38 MAPK in the brain regions of hypoxic preconditioned mice. *Neurochem. Int.* **51**, 459-466.

Calabrese, V., Mancuso, C., Calvani, M., Rizzarelli, E., Butterfield, D. A. and Stella, A. M. G. (2007) Nitric oxide in the central nervous system: neuroprotection versus neurotoxicity. *Nat. Rev. Neurosci.* **8**, 766-775.

Chan, E. D. and Riches, D. W. H. (2001) IFN-γ+LPS induction of iNOS is modulated by ERK, JNK/SAPK, and p38 in a mouse macrophage cell line. *Am. J. Physiol. Cell Physiol.* **280**, C441-C450.

Chitnis, T. and Weiner, H. L. (2017) CNS inflammation and neurodegeneration. *J. Clin. Invest.* **127**, 3577-3587.

Ferruzzi, M. G., Lobo, J. K., Janle, E. M., Cooper, B., Simon, J. E., Wu, Q. L., Welch, C., Ho, L., Weaver, C. and Pasinetti, G. M. (2009) Bioavailability of gallic acid and catechins from grape seed polyphenol extract is improved by repeated dosing in rats: implications for treatment in Alzheimer's disease. *J. Alzheimers Dis.* **18**, 113-124.

Glass, C. K., Saijo, K., Winner, B., Marchetto, M. C. and Gage, F. H. (2010) Mechanisms underlying inflammation in neurodegeneration. *Cell* **140**, 918-934.

Halliwell, B. (2006) Oxidative stress and neurodegeneration: where are we now? *J. Neurochem.* **97**, 1634-1658.

Huang, T. T., Leu, D. and Zou, Y. (2015) Oxidative stress and redox regulation on hippocampal-dependent cognitive functions. *Arch. Biochem. Biophys.* **576**, 2-7.

Jantan, I., Ahmad, W. and Bukhari, S. N. A. (2015) Plant-derived immunomodulators: an insight on their preclinical evaluation and clinical trials. *Front. Plant Sci.* **6**, 655.

Kameyama, T., Nabeshima, T. and Kozawa, T. (1986) Step-down-type passive avoidance-learning and escape-learning method - suitability for experimental amnesia models. *J. Pharmacol. Method* **16**, 39-52.

Kim, S. H. and Shin, T. Y. (2006) Effect of Dracocephalum argunense on mast-cell-mediated hypersensitivity. *Int. Arch. Allergy Immunol.* **139**, 87-95.

Kim, S. R., Park, Y., Li, M., Kim, Y. K., Lee, S., Son, S. Y., Lee, S., Lee, J. S., Lee, C. H., Park, H. H., Lee, J. Y., Hong, S., Cho, Y. C., Kim, J. W., Yoo, H. M., Cho, N., Lee, H. S. and Lee, S. H. (2022) Anti-inflammatory effect of Ailanthus altissima (Mill.) Swingle leaves in lipopolysaccharide-stimulated astrocytes. *J. Ethnopharmacol.* **286**, 114258.

Koeberle, A. and Werz, O. (2014) Multi-target approach for natural products in inflammation. *Drug Discov. Today* **19**, 1871-1882.

Kumar, A. (2018) Editorial: neuroinflammation and cognition. *Front. Aging Neurosci.* **10**, 413.

Kwon, Y. K., Choi, S. J., Kim, C. R., Kim, J. K., Kim, Y. J., Choi, J. H., Song, S. W., Kim, C. J., Park, G. G., Park, C. S. and Shin, D. H. (2016) Antioxidant and cognitive-enhancing activities of Arctium

lappa L. roots in A beta(1-42)-induced mouse model. *Appl. Biol. Chem.* **59**, 553-565.
Lee, K. P., Choi, N. H., Kim, H. S., Ahn, S., Park, I. S. and Lee, D. W. (2018) Anti-neuroinflammatory effects of ethanolic extract of black chokeberry (Aronia melanocapa L.) in lipopolysaccharide-stimulated BV2 cells and ICR mice. *Nutr. Res. Pract.* **12**, 13-19.
Lim, D. W., Park, J., Jung, J., Kim, S. H., Um, M. Y., Yoon, M., Kim, Y. T., Han, D., Lee, C. and Lee, J. (2020) Dicaffeoylquinic acids alleviate memory loss via reduction of oxidative stress in stress-hormone-induced depressive mice. *Pharmacol. Res.* **161**, 105252.
Liu, L., Liu, Y., Zhao, J., Xing, X., Zhang, C. and Meng, H. (2020) Neuroprotective effects of D-(-)-quinic acid on aluminum chloride-induced dementia in rats. *Evid. Based Complement. Alternat. Med.* **2020**, 5602597.
Liu, T. T., Zhu, X. L., Huang, C. L., Chen, J., Shu, S., Chen, G. Q., Xu, Y. and Hu, Y. M. (2022) ERK inhibition reduces neuronal death and ameliorates inflammatory responses in forebrain-specific knockout mice. *FASEB J.* **36**, e22515.
Lu, X., Ma, L., Ruan, L., Kong, Y., Mou, H., Zhang, Z., Wang, Z., Wang, J. M. and Le, Y. (2010) Resveratrol differentially modulates inflammatory responses of microglia and astrocytes. *J. Neuroinflammation* **7**, 46.
Lucas, R. M., Luo, L. and Stow, J. L. (2022) ERK1/2 in immune signalling. *Biochem. Soc. Trans.* **50**,1341-1352.
Park, J. S., Park, E. M., Kim, D. H., Jung, K., Jung, J. S., Lee, E. J., Hyun, J. W., Kang, J. L. and Kim, H. S. (2009) Anti-inflammatory mechanism of ginseng saponins in activated microglia. *J. Neuroimmunol.* **209**, 40-49.
Pittenger, C., Fasano, S., Mazzocchi-Jones, D., Dunnett, S. B., Kandel, E. R. and Brambilla, R. (2006) Impaired bidirectional synaptic plasticity and procedural memory formation in striatum-specific cAMP response element-binding protein-deficient mice. *J. Neurosci.* **26**, 2808-2813.
Rebai, O., Belkhir, M., Sanchez-Gomez, M. V., Matute, C., Fattouch, S. and Amri, M. (2017) Differential molecular targets for neuroprotective effect of chlorogenic acid and its related compounds against glutamate induced excitotoxicity and oxidative stress in rat cortical neurons. *Neurochem. Res.* **42**, 3559-3572.
Reynolds, A., Laurie, C., Mosley, R. L. and Gendelman, H. E. (2007) Oxidative stress and the pathogenesis of neurodegenerative disorders. *Int. Rev. Neurobiol.* **82**, 297-325.
Saha, R. N. and Pahan, K. (2006) Signals for the induction of nitric oxide synthase in astrocytes. *Neurochem. Int.* **49**, 154-163.
Sandiego, C. M., Gallezot, J. D., Pittman, B., Nabulsi, N., Lim, K., Lin, S. F., Matuskey, D., Lee, J. Y., O'Connor, K. C., Huang, Y., Carson, R. E., Hannestad, J. and Cosgrove, K. P. (2015) Imaging robust microglial activation after lipopolysaccharide administration in humans with PET. *Proc. Natl. Acad. Sci. U. S. A.* **112**, 12468-12473.
von Bartheld, C. S., Bahney, J. and Herculano-Houzel, S. (2016) The search for true numbers of neurons and glial cells in the human brain: a review of 150 years of cell counting. *J. Comp. Neurol.* **524**, 3865-3895.
Wang, Z. Q., Wu, D. C., Huang, F. P. and Yang, G. Y. (2004) Inhibition of MEK/ERK 1/2 pathway reduces pro-inflammatory cytokine interleukin-1 expression in focal cerebral ischemia. *Brain Res.* **996**, 55-66.
Zhang, G., He, J. L., Xie, X. Y. and Yu, C. (2012) LPS-induced iNOS expression in N9 microglial cells is suppressed by geniposide via ERK, p38 and nuclear factor-κB signaling pathways. *Int. J. Mol. Med.* **30**, 561-568.
Zhang, Y. J., Wu, L., Zhang, Q. L., Li, J., Yin, F. X. and Yuan, Y. (2011) Pharmacokinetics of phenolic compounds of Danshen extract in rat blood and brain by microdialysis sampling. *J. Ethnopharmacol.* **136**, 129-136.
Zhao, J., Bi, W., Xiao, S., Lan, X., Cheng, X., Zhang, J., Lu, D., Wei, W., Wang, Y., Li, H., Fu, Y. and Zhu, L. (2019) Neuroinflammation induced by lipopolysaccharide causes cognitive impairment in mice. *Sci. Rep.* **9**, 5790.